Supplement of Eur. J. Mineral., 36, 709–719, 2024
https://doi.org/10.5194/ejm-36-709-2024-supplement

European Journal of Mineralogy
Open Access

Supplement of

Dauphiné twin in a deformed quartz: characterization by electron channelling contrast imaging and large-angle convergent-beam diffraction

Nobuyoshi Miyajima et al.

Correspondence to: Nobuyoshi Miyajima (nobuyoshi.miyajima@uni-bayreuth.de)

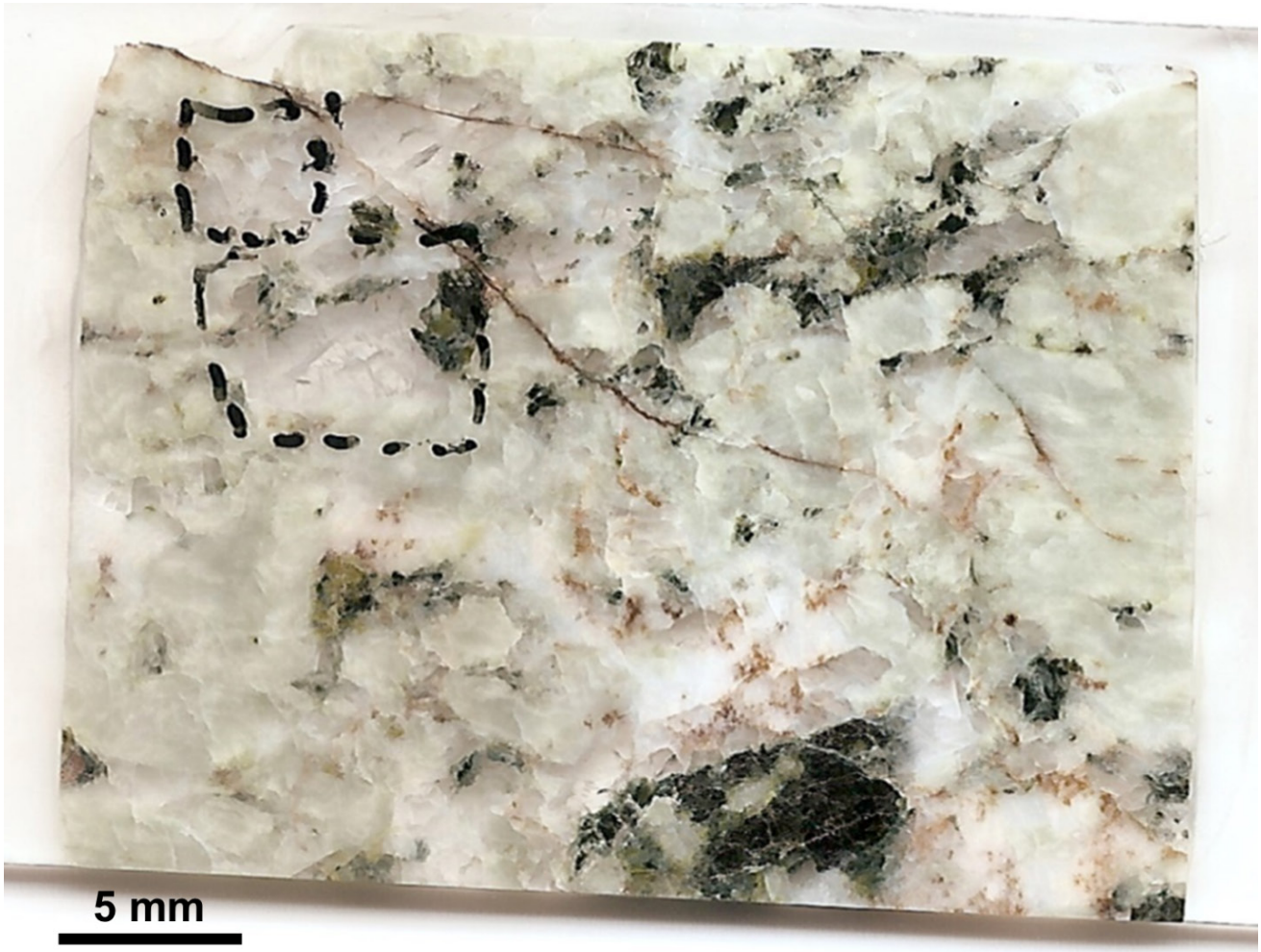

Fig. S1. Optical photomicrograph of a quartzite, quartz porphyroclast in a granitoid protomylonite from the Austro alpine Arolla unit of the Dent Blanche nappe in the north-western Italian Alps (Menegon et al., 2008; 2011), provided with the courtesy of L. Menegon and F. Nestola.

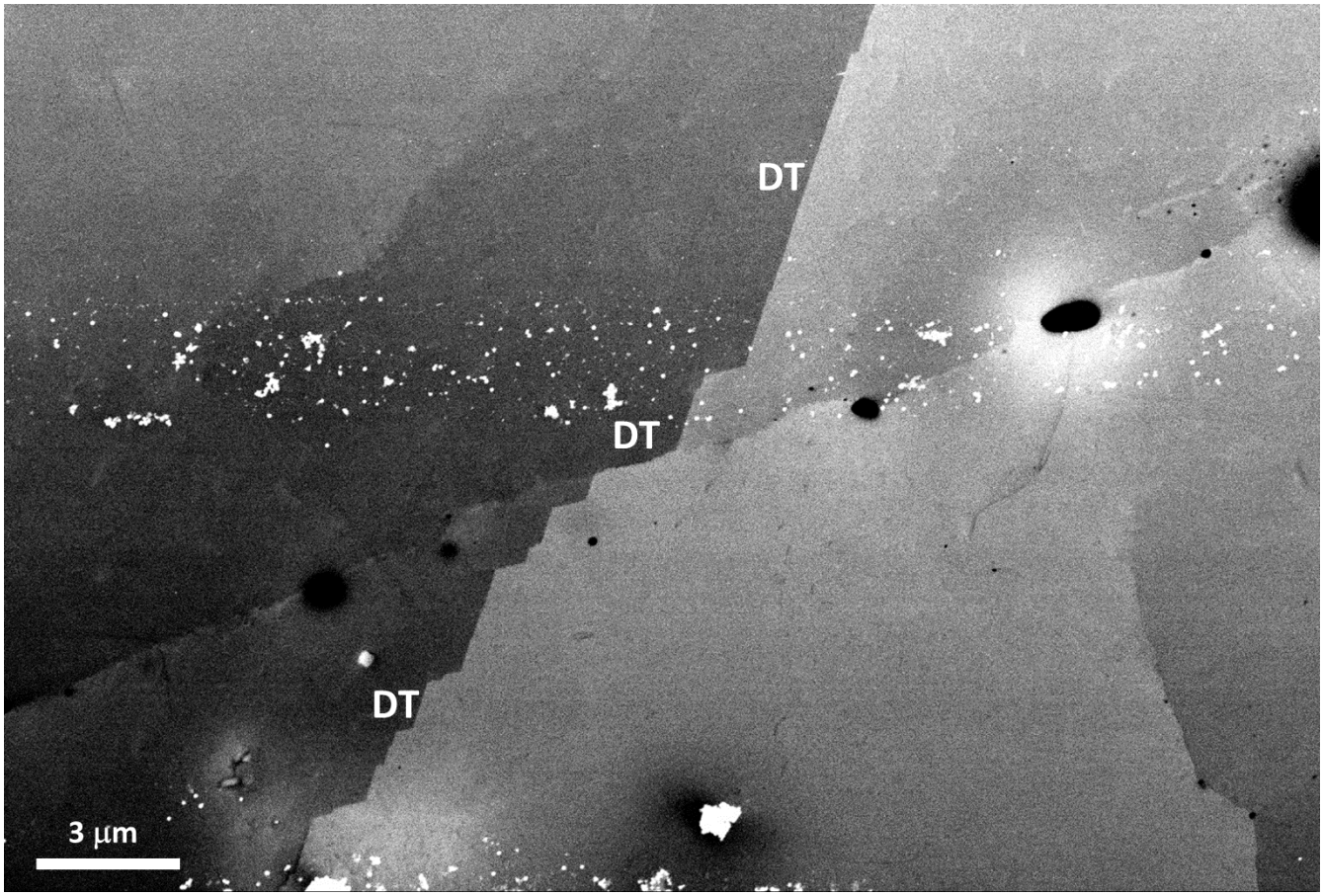

Figure S2: ECCI of a Dauphiné twin boundary separating the black- and white-contrast domains. Individual dislocations are also visible, especially in the upper area. The band consisting of white spheres at the centre is an artefact, the leftover of the final polishing materials (colloidal silica particles).

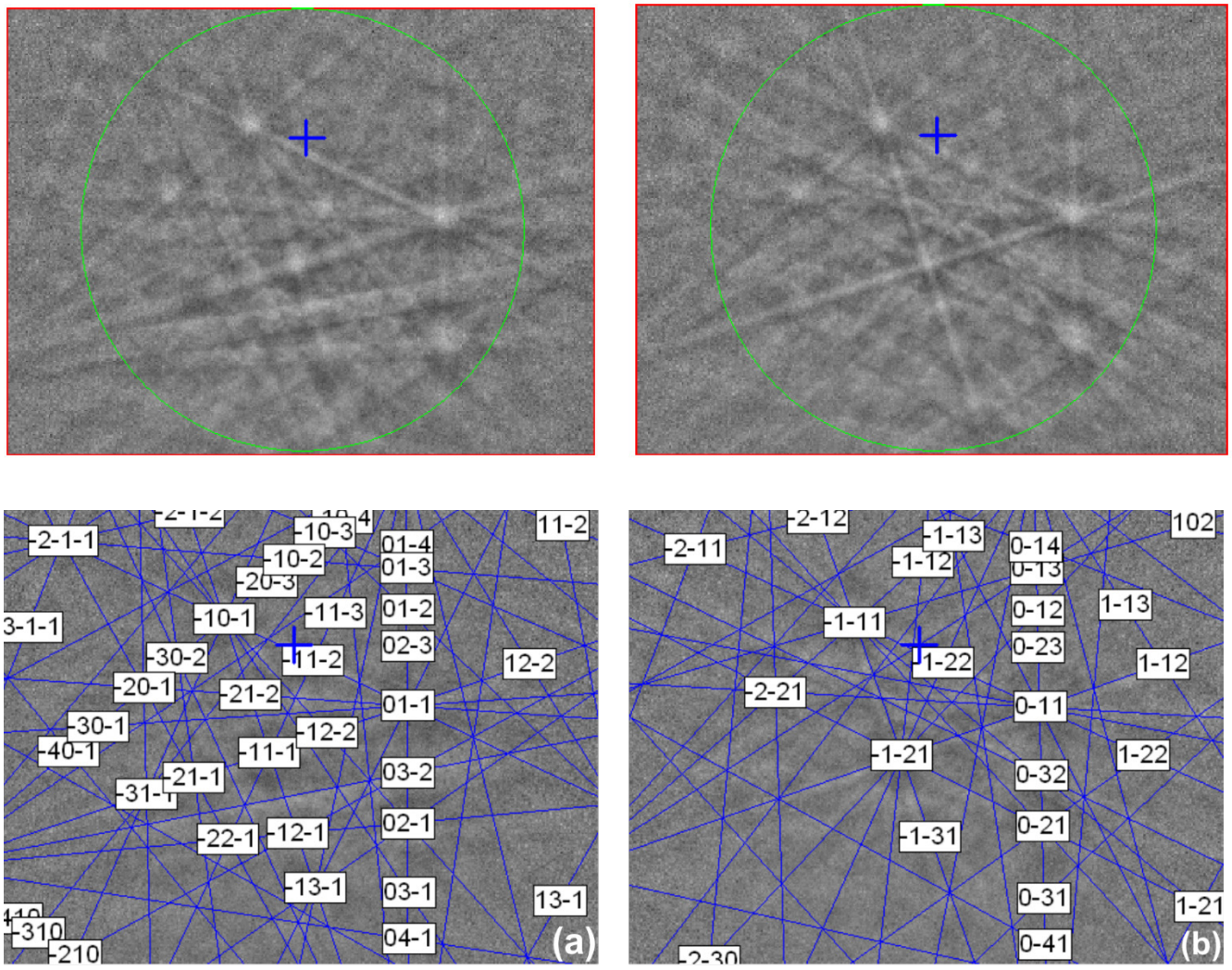

Figure S3: The Kikuchi patterns obtained from (a) the black and (b) white domains indicates a relation of a 180° rotation symmetry along the c-axis in a pair of the Dauphine twins. The raw (upper) and indexed (lower) patterns of zone axes.

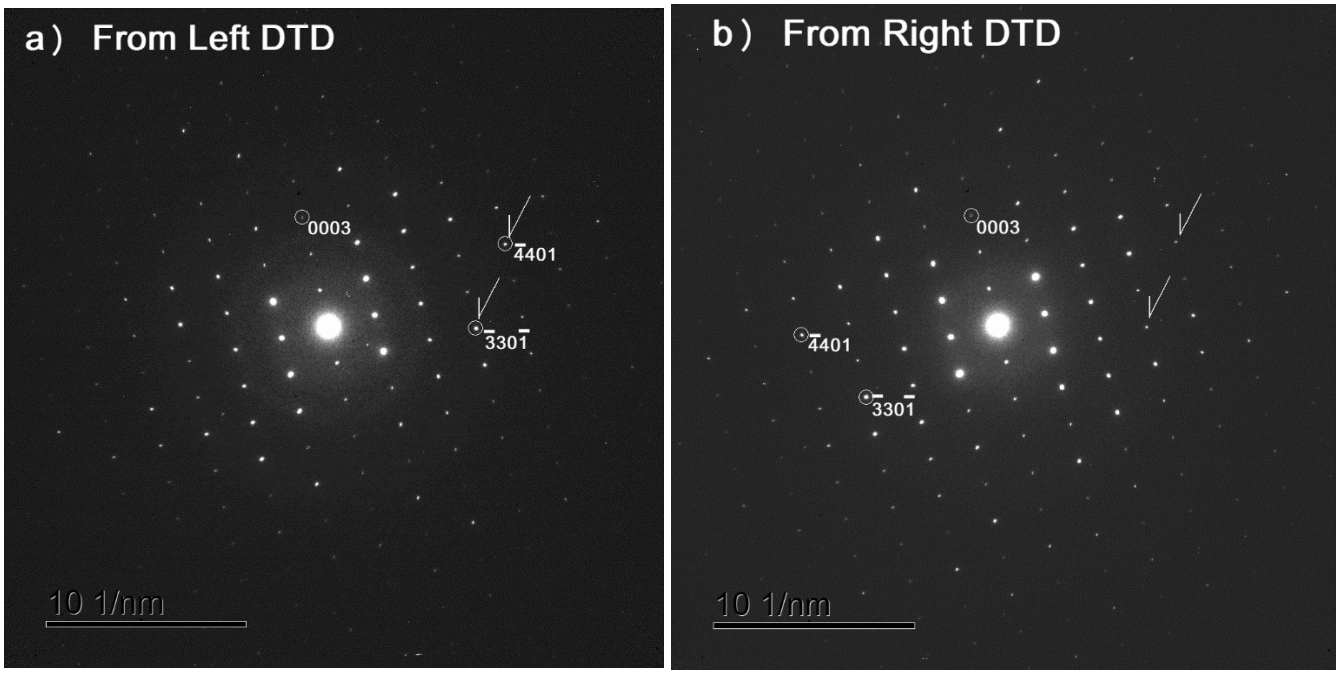

Figure S4: Precession selected area electron diffraction patterns taken separately from the Dauphiné twin domains, (a) Left twin domain and (b) Right twin domain along the <010> zone axis, which indicates different intensities of diffraction spots reflected from the strong ($\bar{3}30\bar{1}$), weak ($\bar{3}301$) and strong ($\bar{4}401$), weak ($\bar{4}40\bar{1}$) rhombohedral planes on the two twin domains. The maximum precession semi-angle is about 3°.

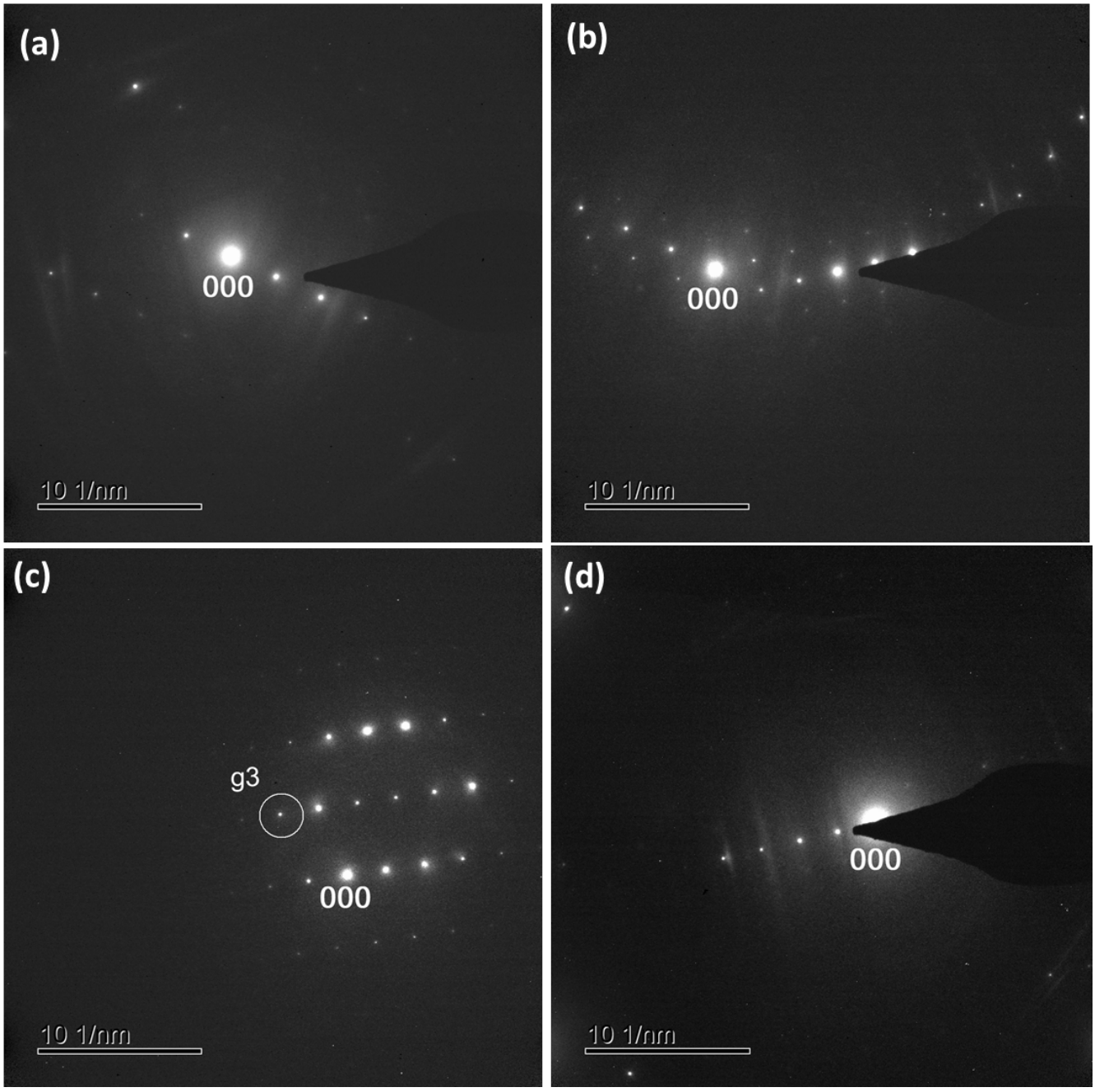

Fig. S5. The diffraction conditions of the dark-field TEM images (Fig. 9) are shown in the corresponding selected area electron diffraction patterns. The *g3* spot corresponds to *g3* = $\bar{2}11\bar{2}$.

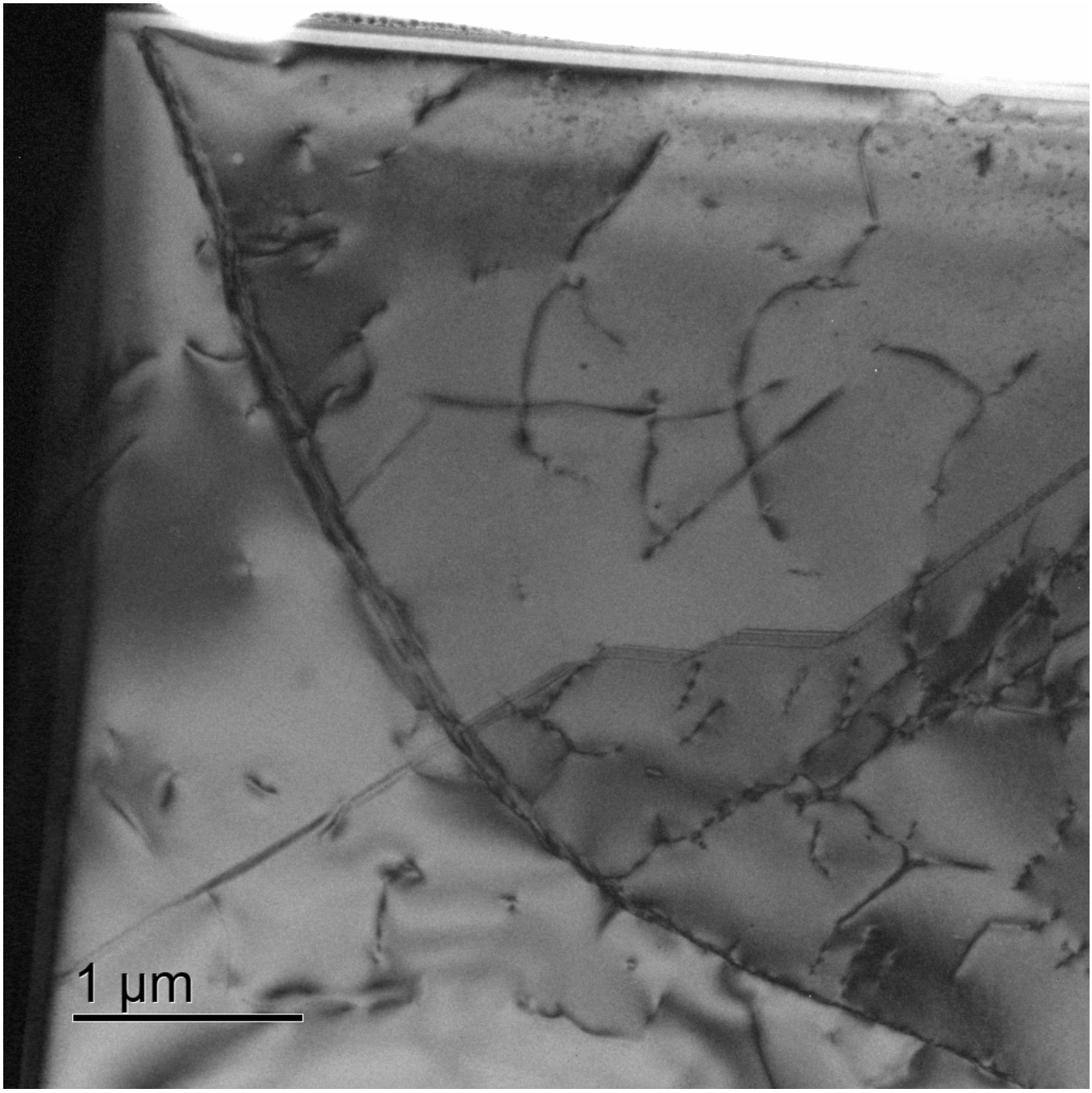

Figure S6(a)

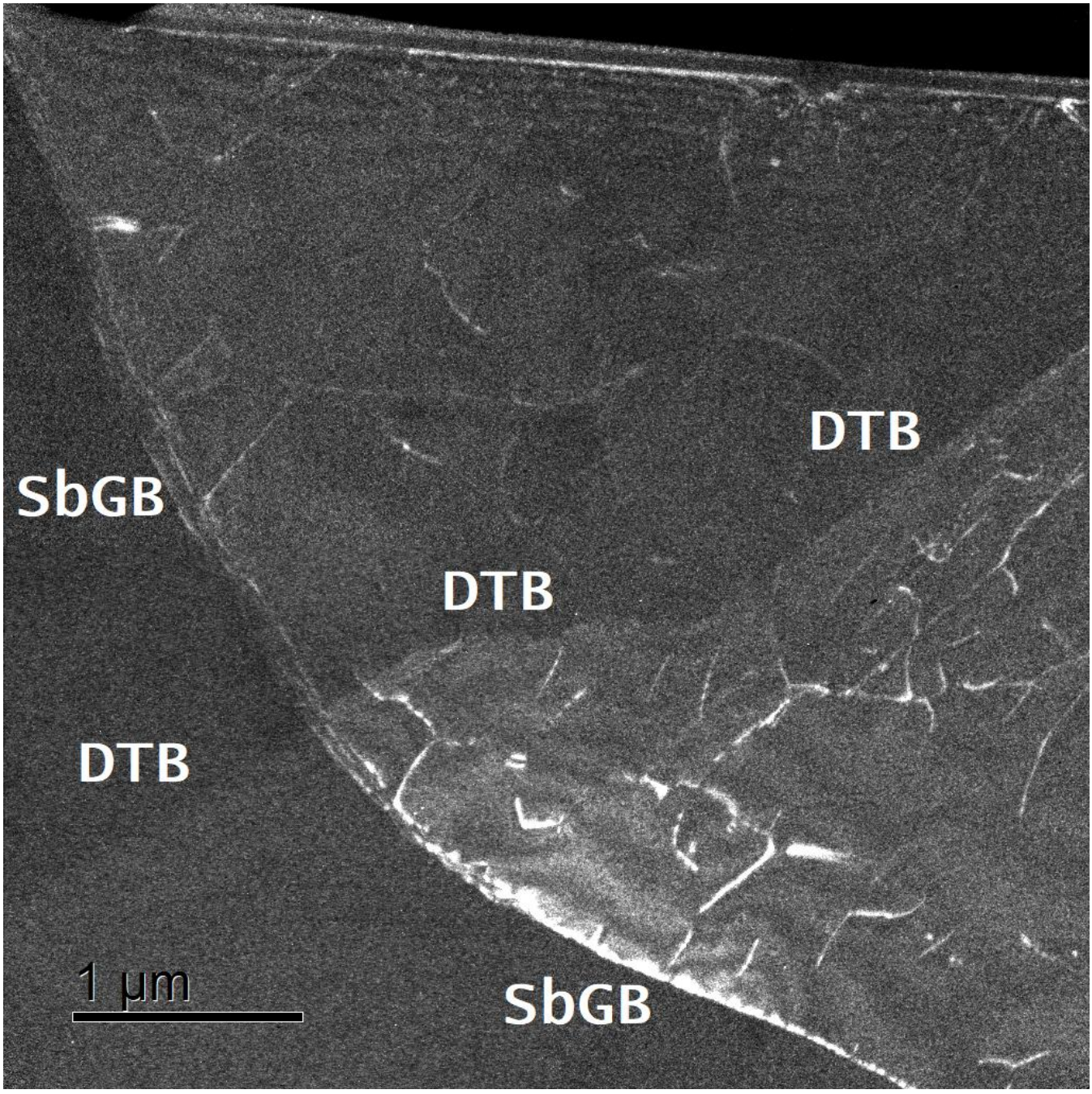

Figure S6(b)

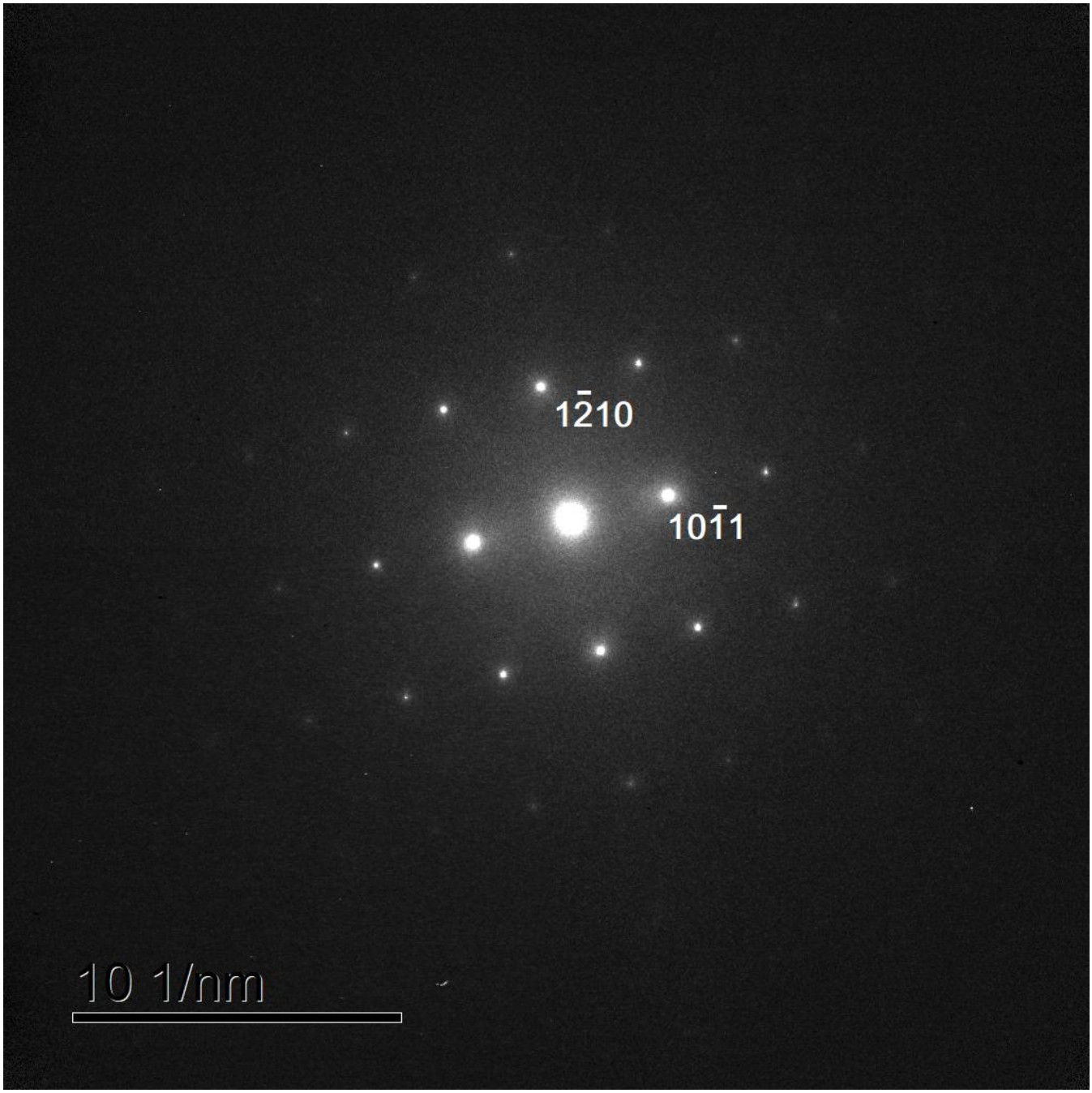

Figure S6(c)

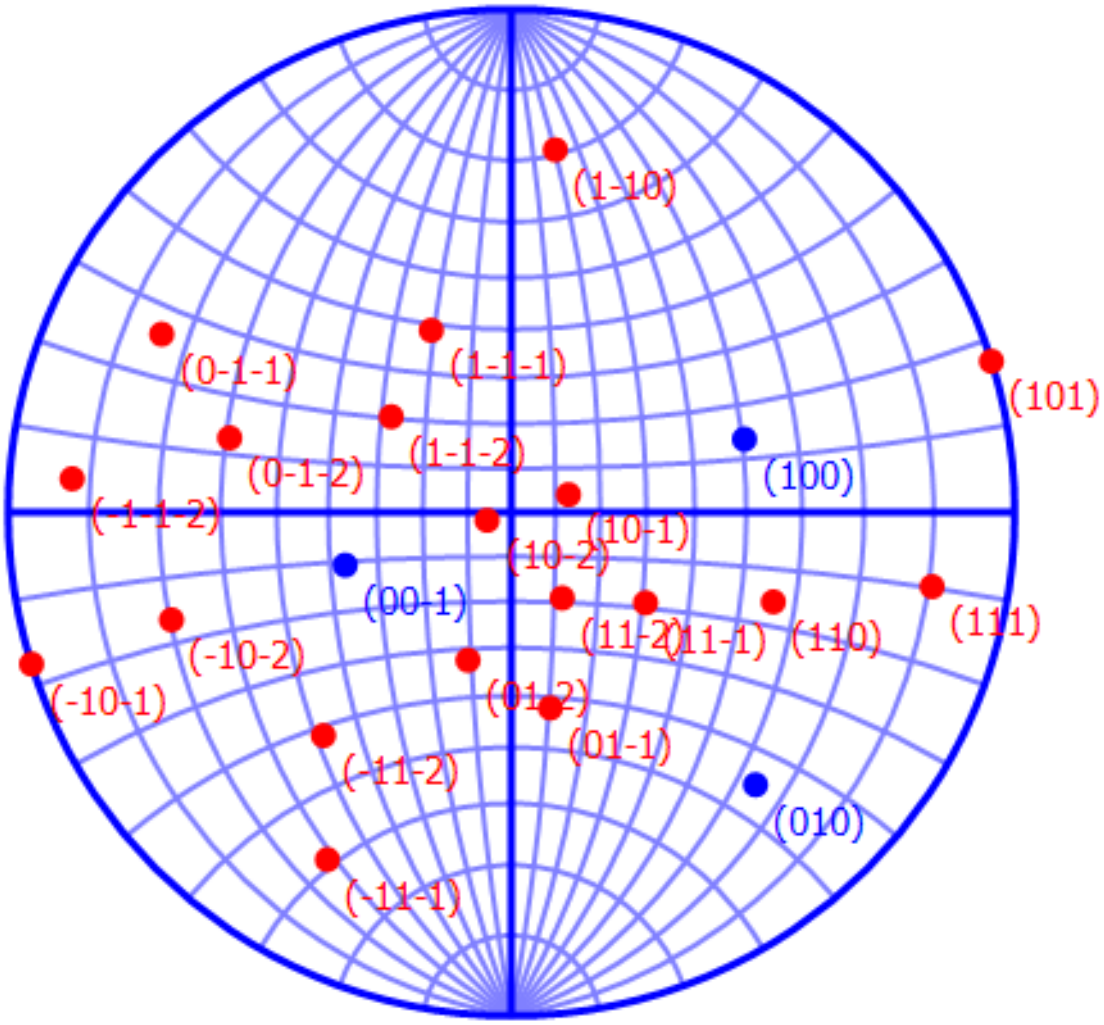

Figure S6 (d)

Figure S6: (a) BF and (b) DF images with $g = 20\bar{2}1$ and $02\bar{2}1$ (s = 0) in different domains having different structure factors in negative and positive rhombohedral planes, respectively, exchanged by a DT. The symbols, DTB and SbGB indicate the positions of a DT boundary and a subgrain boundary, respectively. (c) The SAED pattern of the nearest zone axis corresponding to the images of (a) and (b). (d) The stereo plot of representative planes, made by the ReciPro (Seto and Ohtsuka, 2022).

(a)

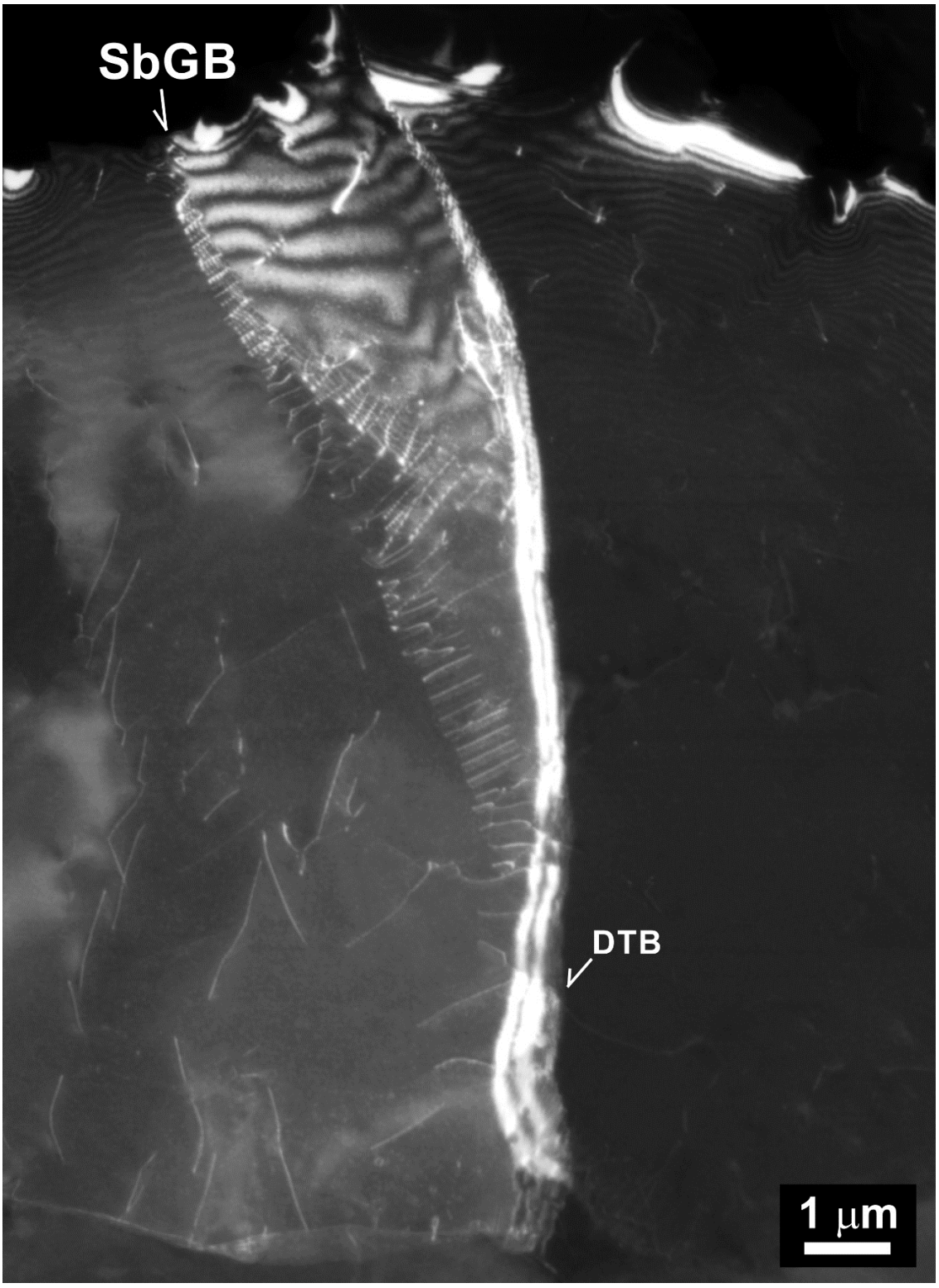

(b)

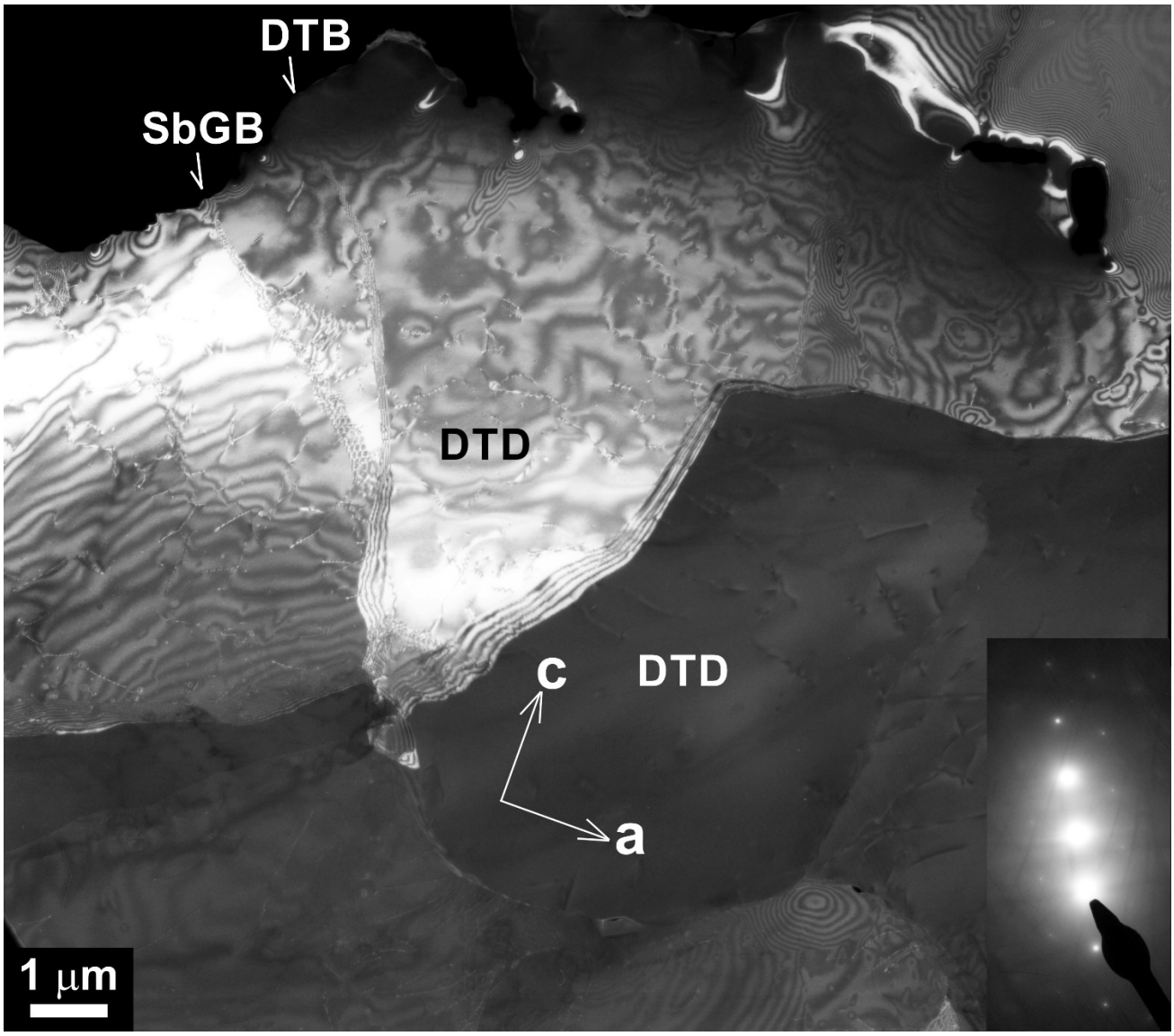

(c)

Figure S7: The interactions of Dauphine twin boundaries (DTB) and subgrain boundaries (SbGB) in a quartz in the same quartzite. (a) The corresponding DF-TEM image (with $g = 10\bar{1}1$) to the Figure 12. The upper irregular boundary is a relic DTB after dislocation pile-ups on the boundary. (b) Close up of the center area of the Figure 13(d). WBDF-TEM image with $g = 30\bar{3}1$. An array of dislocations (SbGB) is stopped at a DTB. (c) The DF-TEM image with $g = 10\bar{1}1$ corresponding to Figure 13(c) and 13(d). The inset is the corresponding SAED pattern. One of Dauphine twin domains (DTD, black characters), the z-twin domain is brighter than the other DTD (white characters), the r-twin domain.

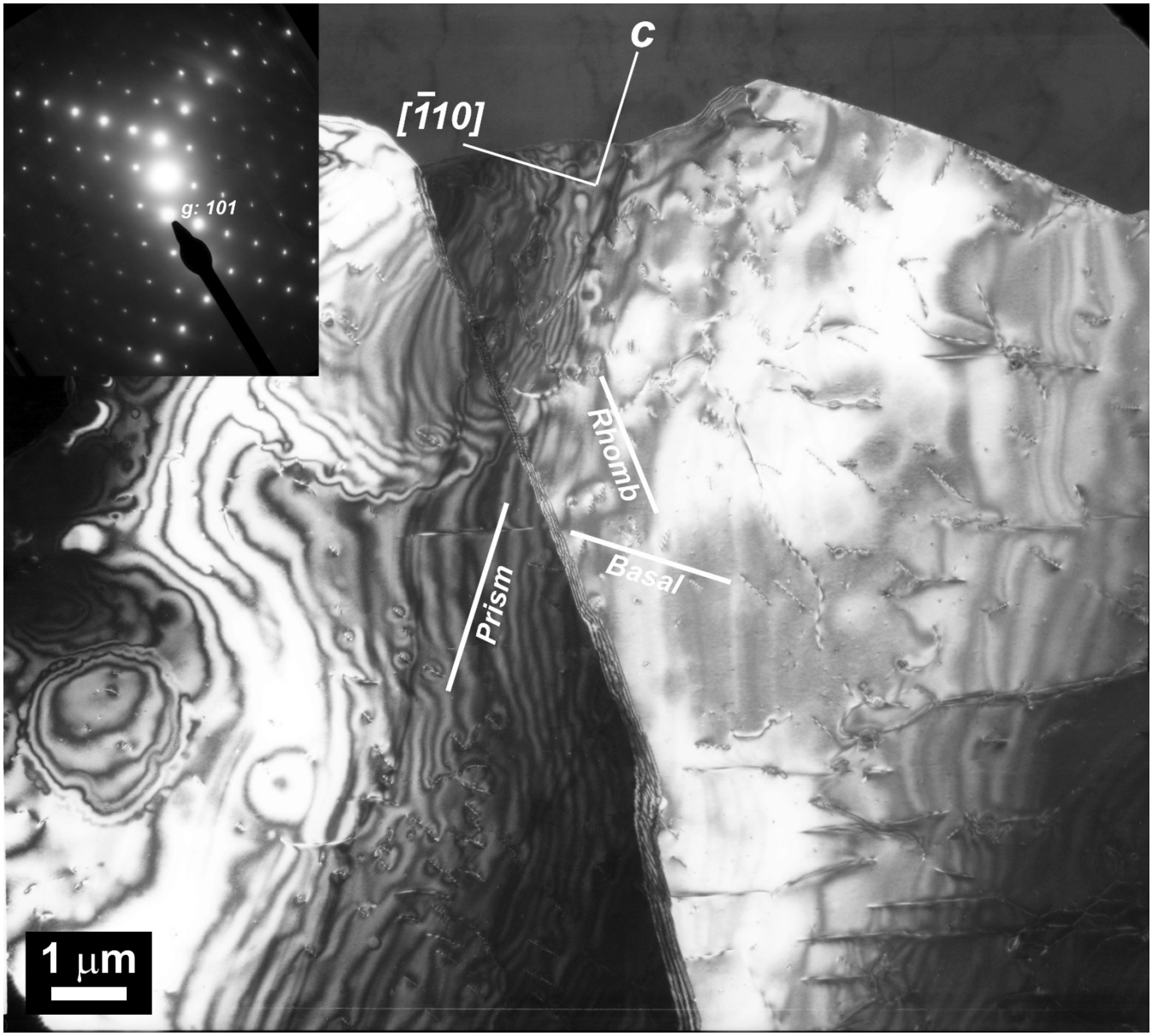

Figure S8: DF-TEM image of a low-angle boundaries of a quartz in the same quartzite. Some long dislocation lines are nearly normal to the c-axis direction, i.e., a slip on the (0001) plane, while the other are on the other slip planes. The inset of the corresponding SAED pattern obtained from the interface between the left and right domains, indicates a misfit angle between those domains, i.e. a low-angle grain boundary with a rotation of the c-axis between them.